Expanded View Figures

Figure EV1. Reduction in BECN1 does not affect IL-6 and TNFalpha release.

A The supernatant of LPS/ATP-treated and non treated wild-type and *Becn1*$^{+/-}$ microglia was probed for the presence of IL-1beta by Western blot, and its expression was normalized on whole protein content of the supernatant (Ponceau staining); mean ± SEM, wild-type $n = 1$, wild-type LPS/ATP $n = 4$, *Becn1*$^{+/-}$ $n = 1$, *Becn1*$^{+/-}$ LPS/ATP $n = 4$, two-tailed *t*-test (LPS/ATP-treated cells) $^{**}P < 0.01$.

B The supernatant of LPS/ATP-treated and non treated wild-type and *Becn1*$^{+/-}$ microglia was probed for the presence of the pro-inflammatory cytokines TNFalpha and IL-6 by ELISA. Reduction in BECN1 did not influence release of these cytokines; mean ± SEM, wild-type $n = 9$; wild-type LPS/ATP $n = 9$; *Becn1*$^{+/-}$ $n = 23$; *Becn1*$^{+/-}$ LPS/ATP $n = 23$, two-tailed *t*-test ns.

C Microglia isolated from wild-type mouse pups were pre-incubated in full medium or starvation medium HBSS before addition of a pro-inflammatory stimulus (LPS followed by ATP). The autophagy blocker 3-MA was added for the final 1 h 45 min of the experiment. The concentration of the cytokines TNFalpha and IL-6 in the cell supernatant was determined by ELISA. Incubation with HBSS reduced cytokine release significantly while 3-MA treatment reduced TNFalpha levels in the supernatant. Mean ± SEM, full medium $n = 3$, full medium LPS/ATP $n = 3$, full medium LPS/ATP + 3-MA $n = 3$, HBSS $n = 3$, HBSS LPS/ATP $n = 3$, HBSS LPS/ATP + 3-MA $n = 3$; two-tailed *t*-test $^{*}P < 0.05$; $^{***}P < 0.001$.

D, E Soluble proteins from the TBS and TX fraction (see Materials and Methods) were extracted from brains of wild-type, *Becn1*$^{+/-}$, *APPPS1*, and *APPPS1 Becn1*$^{+/-}$ mice at the indicated ages, and cytokines were measured by electrochemiluminescence (Meso Scale) and compared within the respective age groups. IL-6 was increased in the TX fraction of 8-month-old mice while TNFalpha was not significantly altered; mean ± SEM, wild-type: *n* (per age group) = 2/6/3; *Becn1*$^{+/-}$: $n = 2/5/2$; *APPPS1*: $n = 5/5/6$; *APPPS1 Becn1*$^{+/-}$: $n = 7/9/6$; ANOVA with Dunnett's post hoc test; $^{*}P < 0.05$.

Source data are available online for this figure.

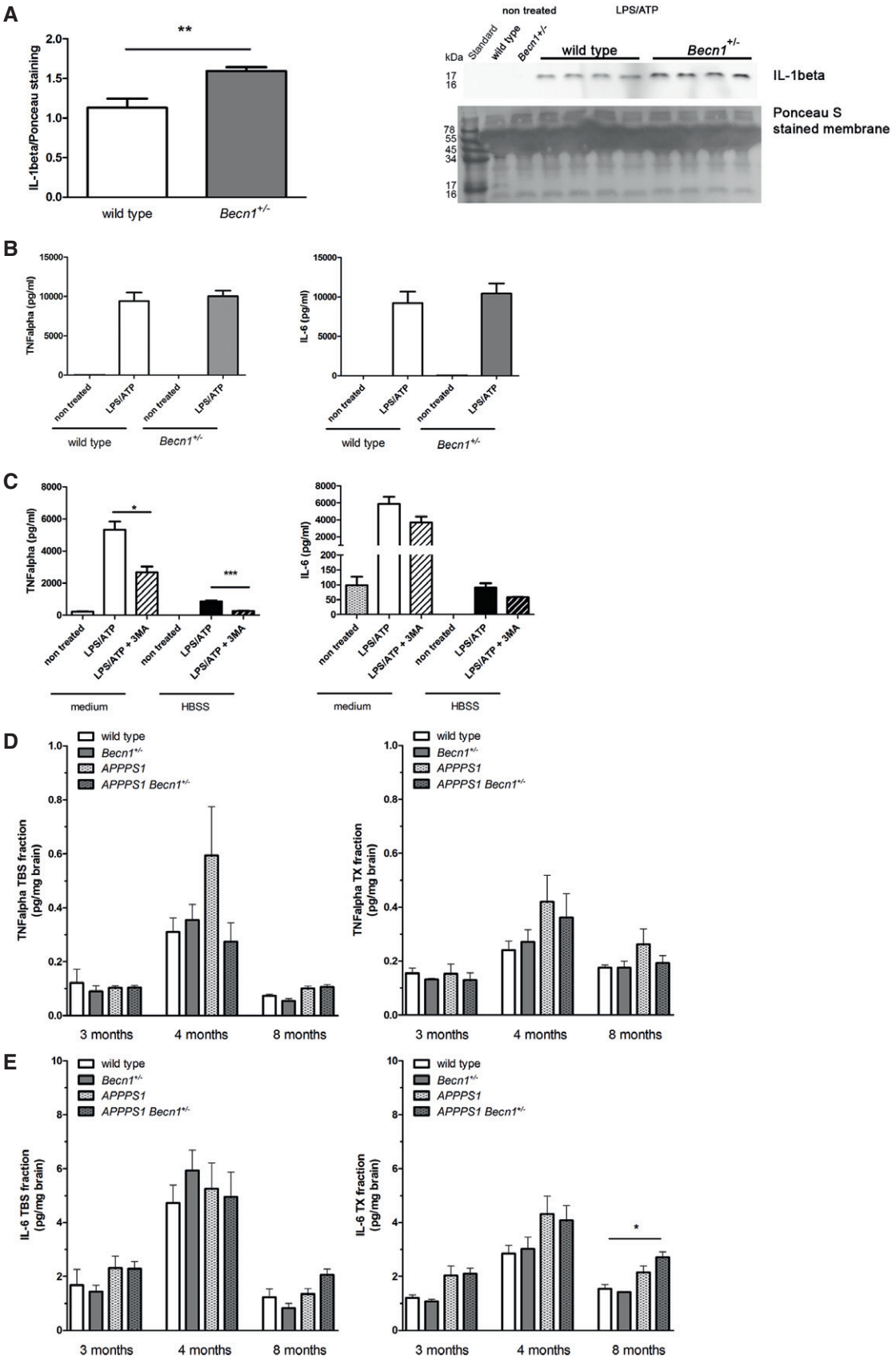
A
IL-1beta/Ponceau staining
wild type
Becn1+/-
non treated
LPS/ATP
Standard
kDa
IL-1beta
Ponceau S stained membrane
B
TNFalpha (pg/ml)
IL-6 (pg/ml)
non treated
LPS/ATP
C
LPS/ATP + 3MA
medium
HBSS
D
APPPS1
APPPS1 Becn1+/-
TNFalpha TBS fraction (pg/mg brain)
TNFalpha TX fraction (pg/mg brain)
3 months
4 months
8 months
E
IL-6 TBS fraction (pg/mg brain)
IL-6 TX fraction (pg/mg brain)

Figure EV1.

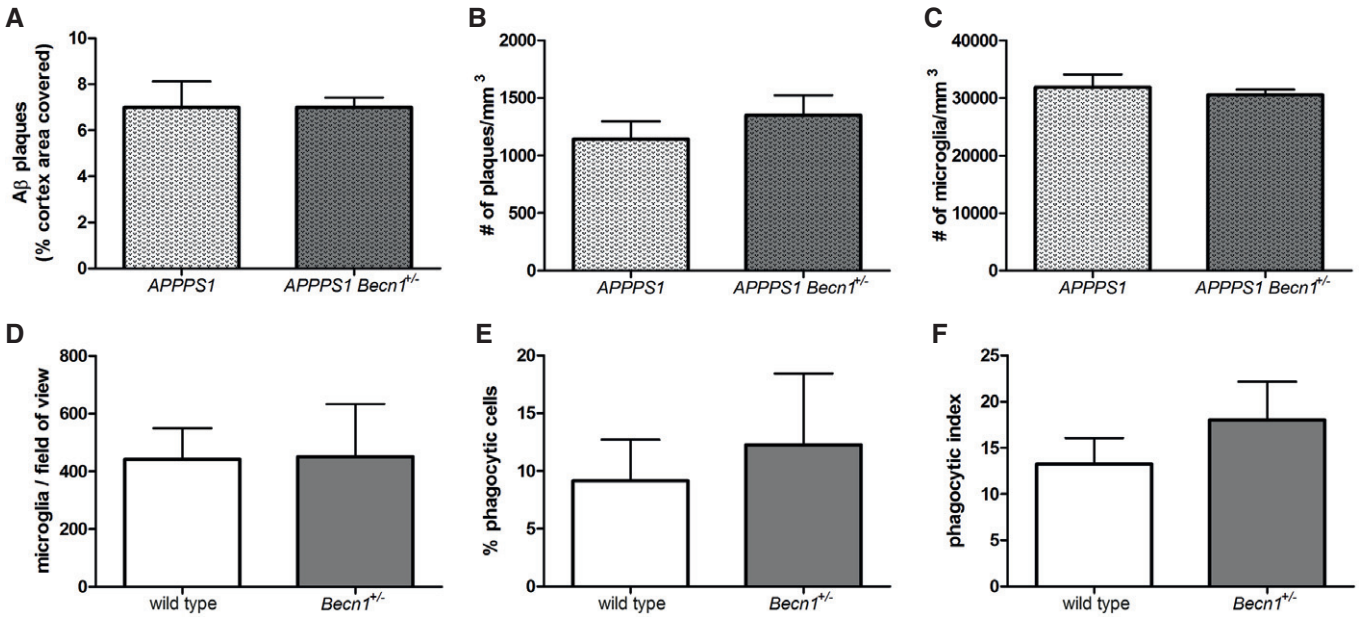

Figure EV2. Abeta pathology and phagocytic capacity are not affected by BECN1 reduction.

A–C Stereological analysis of the cortex of 4-month-old *APPPS1* and *APPPS1-Becn1*$^{+/-}$ mice was performed to assess the area covered by 4G8 (A), the number of core plaques stained with Congo red (B), and the number of Iba1^{+} microglia (C). Mean ± SEM, *APPPS1* n = 4, *APPPS1-Becn1*$^{+/-}$ n = 2, two-tailed t-test ns.

D–F The phagocytosis assay performed in acute brain slices of 4-month-old wild-type and *Becn1*$^{+/-}$ mice was assessed for the number of Iba1^{+} microglia (D), the percentage of phagocytic cells (E), and the phagocytic index (F). Mean ± SEM, wild-type n = 5, *Becn1*$^{+/-}$ n = 4, two-tailed t-test ns.

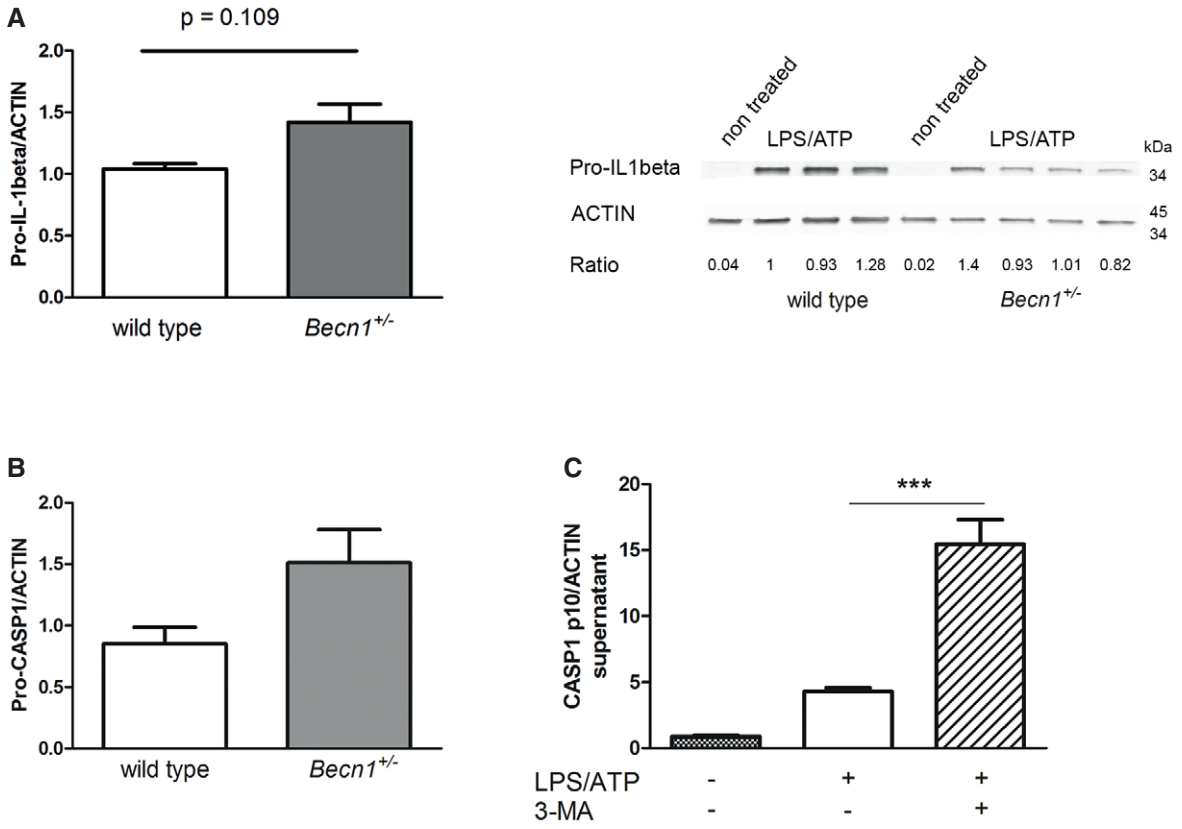

Figure EV3. Decreased autophagy affect levels of activated CASP1, but not IL-1beta or CASP1 precursors.

A Pro-IL-1beta in the cell lysates of LPS/ATP-treated wild-type and *Becn1*$^{+/-}$ microglia was detected by Western blot. No significant differences can be detected between wild-type and *Becn1*$^{+/-}$ microglia; mean ± SEM, wild-type LPS/ATP n = 11, *Becn1*$^{+/-}$ LPS/ATP n = 26, two-tailed t-test ns.

B Pro-CASP1 in LPS/ATP-treated wild-type and *Becn1*$^{+/-}$ microglia was detected by Western blot in the cell lysates. No significant differences can be detected between wild-type and *Becn1*$^{+/-}$ microglia; mean ± SEM, wild-type LPS/ATP n = 6, *Becn1*$^{+/-}$ LPS/ATP n = 14; two-tailed t-test ns.

C Microglia were isolated from newborn wild-type mouse pups and were either non treated or treated with a pro-inflammatory stimulus (LPS followed by ATP) in the presence or absence of 3-MA. The presence of cleaved CASP1 (p10) protein in the cell supernatant was determined by Western blot and normalized to ACTIN. Treatment with 3-MA significantly enhanced the release of CASP1; mean ± SEM, n = 3, ANOVA with Tukey's post hoc test; ***$P < 0.001$.

Source data are available online for this figure.

Figure EV4. Subcellular localization of NLRP3.

A NLRP3 aggregates/μm^2 cell area in LPS/ATP-treated microglia from *Becn1*$^{+/-}$ and wild-type mice (see Fig 4A) were quantified using CLSM images. Analyzing five fields of view (mean ± SEM, n = 1), a significantly higher amount of NLRP3 aggregates was detected in the *Becn1*$^{+/-}$ microglia; two-tailed t-test *$P < 0.05$.

B The 3D distance from NLRP3 aggregates to the nucleus was determined in SIM images of LPS/ATP-treated microglia from *Becn1*$^{+/-}$ and wild-type mice (see Fig 4B). No significant difference between the genotypes was observed; mean ± SEM, wild-type n = 2 (16 fields/view), *Becn1*$^{+/-}$ n = 2 (14 fields/view); two-tailed t-test ns.

C, D LPS/ATP-treated wild-type microglia were immunolabeled for NLRP3 (green) and ASC (red) and imaged with confocal microscopy (CLSM) or structured illumination microscopy (SIM). (C) In CLSM, a partial colocalization of NLRP3 and ASC in stimulated microglia was observed; scale bar: 7.5 μm. (D) 3D volume rendering of NLRP3 aggregates from the magnified ROIs showed that NLRP3 structures corralled around the more central ASC signals; scale bar: 10 μm; magnified ROIs: 1 μm.

E Mitochondria of wild-type cells were stained with MitoTracker Red (MTR) and then stimulated with LPS/ATP. LC3 (purple) and NLRP3 (green) were visualized by immunocytochemistry. Colocalization of NLRP3 with LC3 (white arrow) and colocalizations of NLPR3 with mitochondria (yellow arrow) are visible as well as NLRP3 aggregates/puncta in very close vicinity to the mitochondria but not directly colocalizing (arrowheads); scale bar = 5 μm.

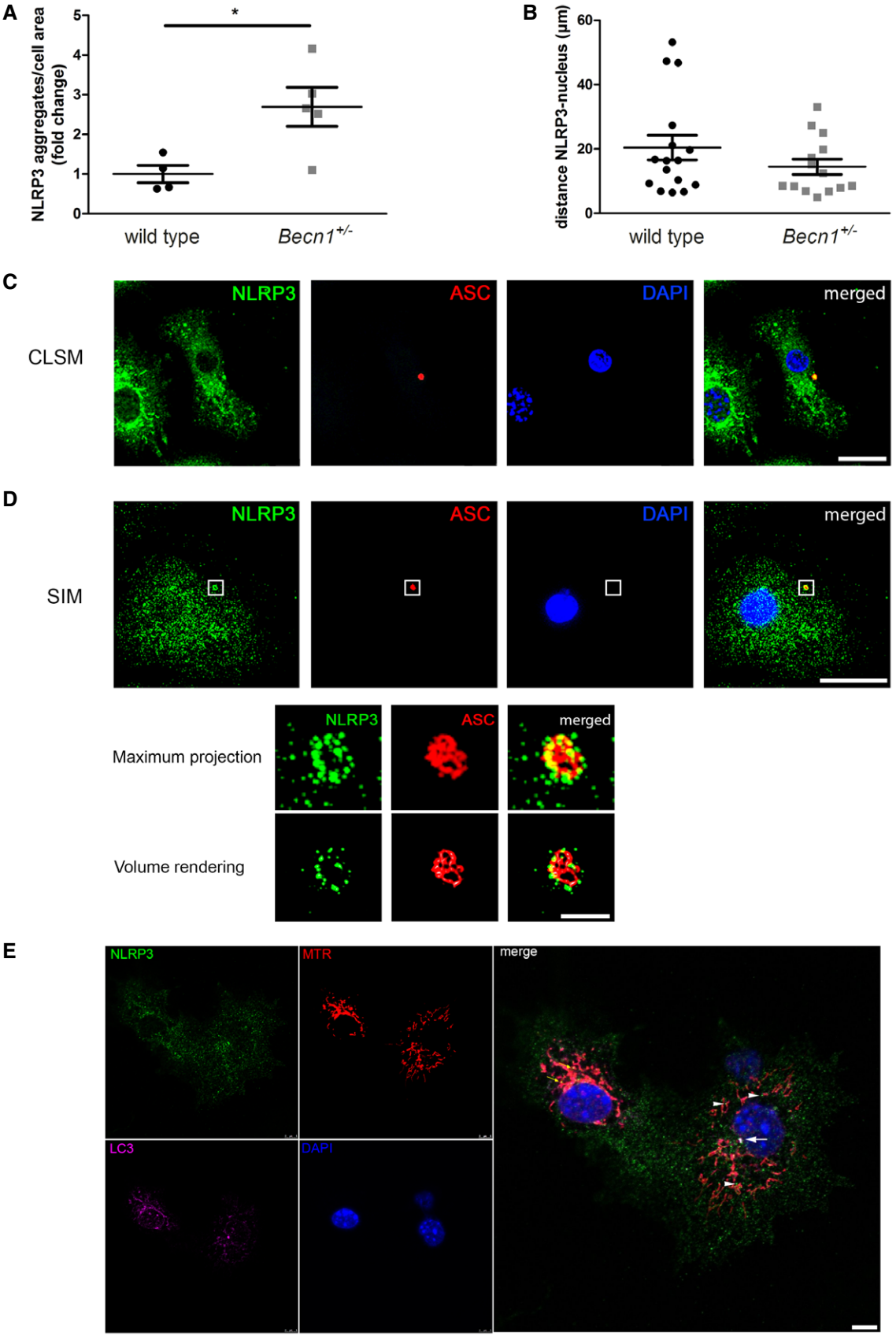

Figure EV4.

Figure EV5. LC3-NLRP3 colocalization is present in adult microglia as well, but not in neonatal astrocytes.

A Adult microglia were isolated from the brains of 8-month-old wild-type and *APPPS1* mice with magnetic beads sorting, stained 4 h after plating on coverslips for NLRP3 (green) and LC3 (red) and observed by confocal microscopy. NLRP3 aggregates (arrows) as well as LC3-NLRP3 colocalization (arrowheads) were found in microglia from both genotypes, confirming that the described *in vitro* phenotype occurs also *in vivo*; scale bar: 10 μm.

B, C Neonatal astrocytes of wild-type and *Becn1*$^{+/-}$ mice do not present NLRP3 upon stimulation with LPS/ATP in Western blot (B), nor in immunocytochemistry (C); scale bar: 25 μm.

D, E Microglia from *Becn1*$^{+/-}$ mice were transfected with a scrambled siRNA or a siRNA for CALCOCO2. 6 d after transfection, cells were stimulated with LPS/ATP. The amount of TNFalpha (D) and IL-6 (E) in the supernatant was determined by ELISA. Microglia with a CALCOCO2 knockdown show no changes in their TNFalpha or IL-6 signals compared to cells transfected with a scrambled siRNA; mean ± SEM, n = 3, two-tailed t-test ns.

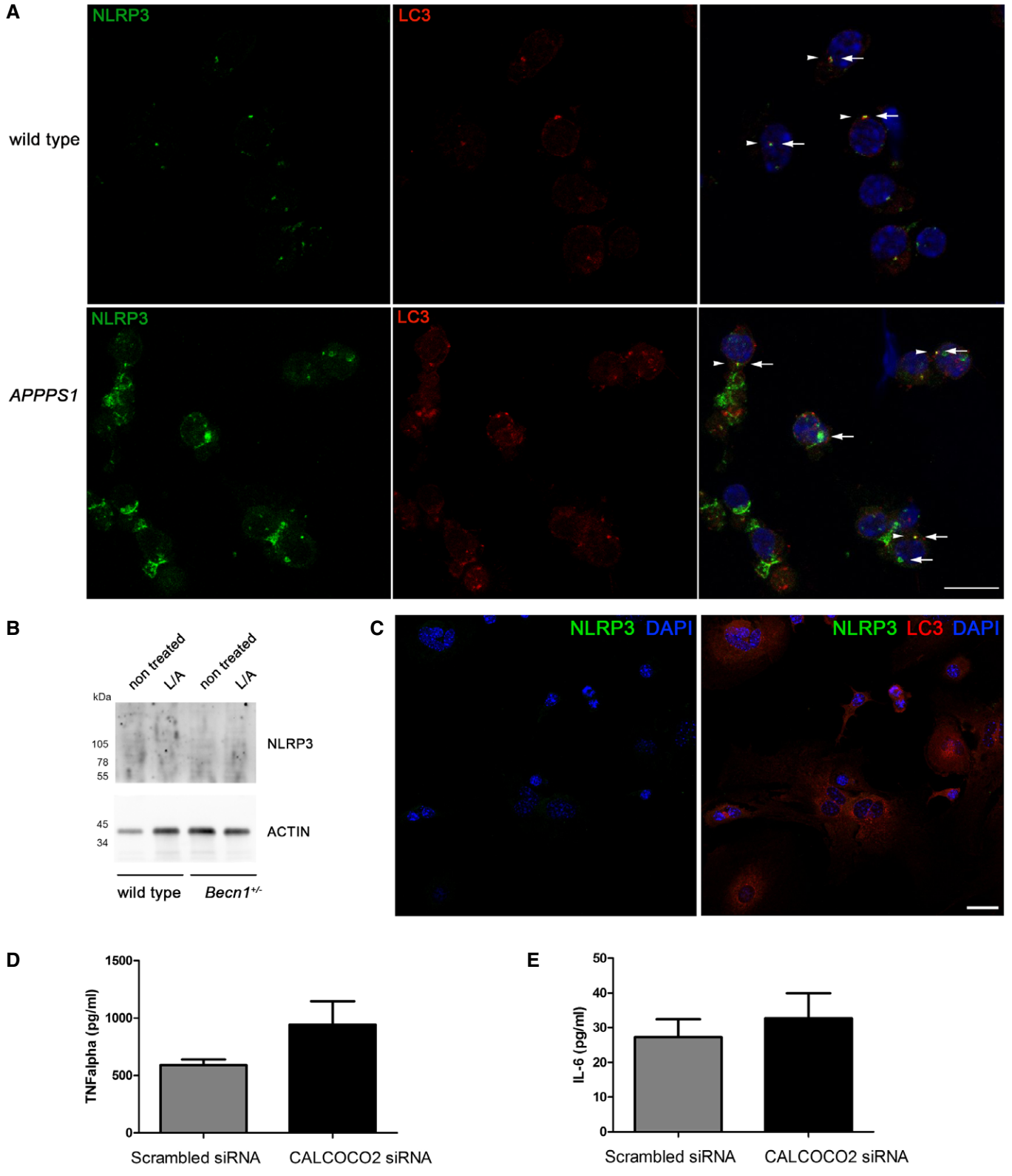

Figure EV5.